

Study of K_{e4} Decays

ROBERT P. ELY, JR., GEORGE GIDAL, VASKEN HAGOPIAN,* AND GEORGE E. KALMUS
Lawrence Radiation Laboratory, University of California, Berkeley, California 94720

AND

KELVIN BILLING, FREDERICK W. BULLOCK, MICHAEL J. ESTEN, M. GOVAN, CYRIL HENDERSON,†
WILLIAM L. KNIGHT,‡ F. RUSSELL STANNARD, AND ORTWIN TREUTLER
Department of Physics, University College London, London, England

AND

UGO CAMERINI, DAVID CLINE, WILLIAM F. FRY, HERMANN HAGGERTY, ROBERT H. MARCH,
AND WILLIAM J. SINGLETON
Department of Physics, University of Wisconsin, Madison, Wisconsin 53706

(Received 16 December 1968)

A study of 13.3×10^6 stopped K^+ in a heavy-liquid bubble chamber yielded 269 K_{e4} decays of the type $e^+\pi^+\pi^-\nu$, a total greater by a factor of 4 than the number found in a previous experiment. No examples of $e^-\pi^+\pi^+\bar{\nu}$ were found. With 95% confidence, the upper limit for the decay rate of $K_{e4}(e^-)$ was found to be 56 sec^{-1} . The rate for $K_{e4}(e^+)$ was found to be $(2.60 \pm 0.30) \times 10^8 \text{ sec}^{-1}$. The angular distributions and the dipion invariant-mass plot have been fitted by varying the form factors f_s , f_p , g , and h , and the difference between s - and p -wave π - π phase shift. Two acceptable solutions have been found. Both agree that the vector form factor h is significantly nonzero and that its sign is negative with respect to that of f_s . Also, it has been found necessary to include f_p in order to obtain a good fit. Although both solutions give the magnitude of the phase difference to be $25 \pm 9 \text{ deg}$, the two estimates have opposite sign. No evidence of a σ resonance is seen. The angular distributions are found to be consistent with time-reversal invariance, and with the locality of lepton production.

I. INTRODUCTION

THE rarity of the K_{e4} decay makes it a difficult process to study. Thus, in spite of its considerable theoretical interest, there has to date been only one experimental investigation,¹ based on 69 events.

The experiment presented here represents an extension of this work with statistics increased by a factor of 4. This has been made possible through the use of a larger heavy-liquid bubble chamber, permitting a greater number of decays per picture. Also the number of pictures taken this time was greater by a factor > 2 .

Progress reports on this work have already been presented at various conferences,² and a preliminary analysis of the data has been given by Berends, Donnachie, and Oades.³

The decay modes of interest are

$$K_{e4}(e^+): K^+ \rightarrow \pi^+\pi^-e^+\nu; \quad (1)$$

$$K_{e4}(e^-): K^+ \rightarrow \pi^+\pi^+e^-\bar{\nu}. \quad (2)$$

The general form of the matrix element has been discussed by several authors,⁴ assuming a $V-A$ theory.⁵ Reaction (2) has been shown to proceed almost entirely through the axial-vector current, whereas reaction (1) is a mixture of vector and axial-vector.

Several interesting topics are investigated in this paper. Firstly, the $\Delta Q = \Delta S$ selection rule forbids $K_{e4}(e^-)$, so a search for this reaction permits a test of the rule for axial-vector currents in weak interactions.^{4,6} The rate for $K_{e4}(e^+)$ is compared with several predictions,^{4,6-11} some of which include the effects of final-state interactions.

The angular correlations between the decay products lead to a determination of the form factors, and these are checked against theoretical prediction.¹¹ They also permit a test of time-reversal invariance.

⁴ V. S. Mathur, *Nuovo Cimento* **14**, 1322 (1959); L. B. Okun and E. P. Shabalin, *Zh. Eksperim. i Teor. Fiz.* **37**, 1775 (1959) [English transl.: *Soviet Phys.—JETP* **10**, 1252 (1960)]; A. Sirlin, *Phys. Rev.* **129**, 1377 (1963).

⁵ R. P. Feynman and M. Gell-Mann, *Phys. Rev.* **109**, 193 (1958).

⁶ K. Chadan and S. Oneda, *Phys. Rev. Letters* **3**, 292 (1959); E. P. Shabalin, *Zh. Eksperim. i Teor. Fiz.* **39**, 345 (1960) [English transl.: *Soviet Phys.—JETP* **12**, 245 (1961)]; R. E. Berends and A. Sirlin, *Phys. Rev. Letters* **8**, 221 (1962); B. Sakita, M. Kato, and E. McClement, University of Wisconsin Report (unpublished); B. A. Arbazov, Nguyen Van Hieu, and R. N. Faustov, *Zh. Eksperim. i Teor. Fiz.* **44**, 329 (1963) [English transl.: *Soviet Phys.—JETP* **17**, 225 (1963)].

⁷ J. Iliopoulos, *Orsay Report No. TH/84* (unpublished); and Erratum (unpublished).

⁸ G. Ciocchetti, *Nuovo Cimento* **25**, 385 (1962).

⁹ L. M. Brown and H. Faier, *Phys. Rev. Letters* **12**, 514 (1964).

¹⁰ C. Kacser, P. Singer, and T. N. Truong, *Phys. Rev.* **137**, B1605 (1965); **139**, AB5(E) (1965).

¹¹ S. Weinberg, *Phys. Rev. Letters* **17**, 336 (1966); **18**, 1178(E) (1967).

* Present address: University of Pennsylvania.

† Present address: University of Aberdeen.

‡ Present address: CERN.

¹ R. W. Birge, R. P. Ely, Jr., G. Gidal, G. E. Kalmus, A. Kernan, W. M. Powell, U. Camerini, D. Cline, W. F. Fry, J. G. Gaidos, D. Murphree, and C. T. Murphy, *Phys. Rev.* **139**, B1600 (1965).

² *Proceedings of the Thirteenth International Conference on High-Energy Physics, Berkeley, 1966* (University of California Press, Berkeley, 1967); Meeting of the Physical Society and Institute of Physics, held at University College, London, 1967 (unpublished); Princeton Conference on K Mesons, 1967 (unpublished); *Proceedings of the Fourteenth International Conference on High-Energy Physics, Vienna, 1968* (CERN, Geneva, Switzerland, 1968).

³ F. A. Berends, A. Donnachie, and G. C. Oades, *Nucl. Phys.* **B3**, 569 (1967).

Lastly, K_{e4} decays are notable for their unique property of allowing one to investigate the s -wave $\pi\pi$ interaction in the absence of any additional strongly interacting particles.¹²⁻¹⁶ This arises because in the final state of the decay, the two pions are accompanied only by two leptons.

II. THEORY

In this section we are following the treatment of the theory given in a paper by Pais and Treiman.¹⁶

The matrix element in first-order perturbation theory (aside from the usual kinematic factors) is

$$M[K_{e4}(e^+)] = |G/\sqrt{2}| [\bar{\nu}\gamma^\lambda(1+\gamma_5)e] \times \langle \pi^+\pi^- | J_\lambda^V + J_\lambda^A | K^+ \rangle,$$

where J^V and J^A are the strangeness-changing vector and axial-vector currents of the hadrons.

From invariance considerations

$$\langle \pi^+\pi^- | J_\lambda^V | K^+ \rangle = (h/M^3) \epsilon_{\lambda\mu\nu\sigma} K_\mu P_\nu Q_\sigma$$

and

$$\langle \pi^+\pi^- | J_\lambda^A | K^+ \rangle = (1/M) [fP_\lambda + gQ_\lambda + r(K-P)_\lambda],$$

where M is the mass of the K meson, and $P = (p_+ + p_-)$, $Q = (p_+ - p_-)$, where p_+ and p_- are the π^+ and π^- four-momenta and K is the kaon four-momentum. The dimensionless form factors, f , g , r , and h , are functions of the invariant quantities P^2 , $(K-P)^2$, and $(K \cdot Q)$, or equivalently, S_π , S_l , and θ_π , where S_π is the square of the $\pi^+\pi^-$ invariant mass (i.e., $S_\pi = -P^2$) and S_l is the square of the $e^+\nu$ invariant mass (i.e., $S_l = -L^2$, where $L = p_e + p_\nu$; p_e and p_ν are the positron and neutrino four-momenta). In Fig. 1 we have the definition of θ_π , which is the angle of the π^+ in the dipion center-of-mass system with respect to the dipion line of flight.

Apart from spin, K_{e4} decay is kinematically parameterized by five independent variables. We have chosen these five to be S_π , S_l , θ_π , θ_l , and ϕ . The latter two angles are also defined in Fig. 1.

The probability distribution summed over lepton spins is of the form

$$d^5W = \frac{\pi^2 G^2 \sin^2 \theta_C}{(2\pi)^8 16 M^5} X \left(\frac{Q^2}{S_\pi} \right)^{1/2} \left(1 - \frac{m^2}{S_l} \right)^2 I(S_\pi, S_l, \theta_\pi, \theta_l, \phi) \times dS_\pi dS_l d\cos\theta_\pi d\cos\theta_l d\phi, \quad (3)$$

where θ_C is the Cabbibo angle, m is the electron mass, and X is defined as $X = [(P \cdot L)^2 - S_\pi \cdot S_l]^{1/2}$.

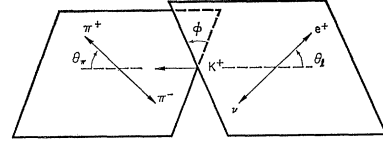


FIG. 1. Diagram illustrating the various angles referred to in the text.

The distribution function I has an explicit structure in the variables θ_l and ϕ , which do not enter into the form factors. By grouping terms according to their behavior with respect to these variables we can examine the spectra more readily.

For I we have

$$I = I_1 + I_2 \cos 2\theta_l + I_3 \sin^2 \theta_l \cos 2\phi + I_4 \sin 2\theta_l \cos \phi + I_5 \sin \theta_l \cos \phi + I_6 \cos \theta_l + I_7 \sin \theta_l \sin \phi + I_8 \sin 2\theta_l \sin \phi + I_9 \sin^2 \theta_l \sin 2\phi. \quad (4)$$

Neglecting terms involving m^2/S_l , the functions $I_1 \cdots I_9$ depend on S_π , S_l , and θ_π , in the following manner (for the complete expressions see Ref. 16):

$$\begin{aligned} I_1 &= \frac{1}{4} [|F_1|^2 + \frac{3}{2} \sin^2 \theta_\pi (|F_2|^2 + |F_3|^2)], \\ I_2 &= -\frac{1}{4} [|F_1|^2 - \frac{1}{2} \sin^2 \theta_\pi (|F_2|^2 + |F_3|^2)], \\ I_3 &= -\frac{1}{4} [|F_2|^2 - |F_3|^2] \sin^2 \theta_\pi, \\ I_4 &= \frac{1}{2} \operatorname{Re} F_1^* F_2 \sin \theta_\pi, \\ I_5 &= -\operatorname{Re} F_1^* F_3 \sin \theta_\pi, \\ I_6 &= -\operatorname{Re} F_2^* F_3 \sin^2 \theta_\pi, \\ I_7 &= -\operatorname{Im} F_1^* F_2 \sin \theta_\pi, \\ I_8 &= \frac{1}{2} \operatorname{Im} F_1^* F_3 \sin \theta_\pi, \\ I_9 &= -\frac{1}{2} \operatorname{Im} F_2^* F_3 \sin^2 \theta_\pi. \end{aligned} \quad (5)$$

F_1 , F_2 , and F_3 are the following combinations of kinematic factors and form factors:

$$\begin{aligned} F_1 &= X f - (P \cdot L) (Q^2/S_\pi)^{1/2} g \cos \theta_\pi, \\ F_2 &= (Q^2 S_l)^{1/2} g, \\ F_3 &= (Q^2 S_l)^{1/2} X (h/M^2). \end{aligned} \quad (6)$$

Note that the r form factor is unimportant in K_{e4} decay, as it is always multiplied by m^2/S_l , and so does not appear in (6).

The form factors f , g , and h carry direct strong-interaction information, assuming time-reversal invariance holds. In a partial-wave expansion of the form factors with respect to the angular momentum of the dipion system, a partial-wave amplitude of definite angular momentum and isospin must have the phase of the corresponding pion-pion scattering amplitude. The odd partial waves have $I=1$ for the dipion system, whereas even partial waves contribute to both $I=0$ and $I=2$ states. Invoking the $\Delta I = \frac{1}{2}$ rule for semileptonic decays, we are left with $l=0$, $I=0$, and $l=1$, $I=1$ states, assuming that states with $l \geq 2$ are not important at these low energies.

¹² E. P. Shabalin, Zh. Eksperim. i Teor. Fiz. 44, 765 (1963) [English transl.: Soviet Phys.—JETP 17, 517 (1963)].

¹³ N. Cabibbo and A. Maksymowicz, Phys. Rev. 137, B438 (1965); 168, 1926(E) (1968).

¹⁴ R. H. Dalitz, in *Proceedings of the International School of Physics "Enrico Fermi," Varenna Lectures* (Academic Press Inc., New York, 1964).

¹⁵ S. Weinberg, Phys. Rev. Letters 17, 616 (1966).

¹⁶ A. Pais and S. B. Treiman, Phys. Rev. 168, 1858 (1968).

The terms in the partial-wave expansion up to and including $l=1$ can now be written

$$\begin{aligned} f &= \tilde{f}_s e^{i\delta s} + \tilde{f}_p e^{i\delta p} \cos\theta_\pi, \\ g &= \tilde{g} e^{i\delta p}, \\ h &= \tilde{h} e^{i\delta p}, \end{aligned} \quad (7)$$

where \tilde{f}_s , \tilde{f}_p , \tilde{g} , and \tilde{h} are real functions of the variables S_π and S_l , and the phases δs and δp are the pion-pion phase shifts, and are functions of S_π .

By substituting (7) into (6) we obtain

$$\begin{aligned} F_1 &= X \tilde{f}_s e^{i\delta s} + X \tilde{f}_p e^{i\delta p} \cos\theta_\pi \\ &\quad - (P \cdot L) (Q^2/S_\pi)^{1/2} \tilde{g} e^{i\delta p} \cos\theta_\pi, \\ F_2 &= (Q^2 S_l)^{1/2} \tilde{g} e^{i\delta p}, \\ F_3 &= (Q^2 S_l)^{1/2} X (\tilde{h} e^{i\delta p}/M^2). \end{aligned} \quad (8)$$

This is a perfectly valid substitution as long as \tilde{f}_s , \tilde{f}_p , \tilde{g} , and \tilde{h} are functions of S_π and S_l . In the case of the p -wave form factors \tilde{f}_p , \tilde{g} , and \tilde{h} , however, there is a known energy dependence due to the angular momentum barrier, which may be explicitly taken out of the form factors. In fact this has been done for \tilde{g} and \tilde{h} , but not yet for \tilde{f}_p . To do this for \tilde{f}_p we somewhat arbitrarily substitute $\beta X \tilde{f}_p'/M^2$, where $\beta \equiv (Q^2/S_\pi)^{1/2}$. The exact form the expressions should take is unknown, but our choice has the essential feature of forcing \tilde{f}_p to zero when S_π equals $4\mu^2$, where μ is the mass of the pion. Therefore,

$$\begin{aligned} F_1 &= X \tilde{f}_s e^{i\delta s} + (\beta X^2/M^2) \tilde{f}_p' e^{i\delta p} \cos\theta_\pi \\ &\quad - (P \cdot L) \beta \tilde{g} e^{i\delta p} \cos\theta_\pi. \end{aligned} \quad (8')$$

By substituting Eqs. (8) and (8') into (5) we obtain the distribution function I in terms of kinematic factors, the form factors \tilde{f}_s , \tilde{f}_p' , \tilde{g} , \tilde{h} , and the s - and p -wave phase shifts δs and δp . In fact, since the absolute phase is arbitrary, the difference of the phases $(\delta s - \delta p)$ is the measured quantity.

In this treatment we have assumed that the leptons are produced at a point. This implies that the θ_l distribution can be fitted by an expression of the form

$$dW/d \cos\theta_l = A(1 + B \cos\theta_l + C \cos 2\theta_l), \quad (9)$$

and the ϕ distribution is fitted by

$$dW/d\phi = \alpha(1 + \beta \cos\phi + \gamma \sin\phi + \delta \sin^2\phi + \epsilon \sin 2\phi) \quad (10)$$

[these distributions are obtained by integrating (3) over all variables except θ_l and ϕ].

Should extra terms be needed in either of these distributions, this would be a violation of the assumption of locality for the lepton production.

Four approaches were used in the analysis of the data from this experiment.

A. First Method

Expression (3) was used to generate Monte Carlo K_{e4} events for particular values of ν ($\equiv \tilde{f}_p'/\tilde{f}_s$), η ($\equiv \tilde{g}/\tilde{f}_s$),

and γ ($\equiv \tilde{h}/\tilde{f}_s$), and of a_0 , where a_0 is related to the s -wave phase shift by the Chew-Mandelstam effective range formula,

$$\cot\delta s = \frac{1}{a_0\beta} + \frac{2}{\pi} \ln \left[\frac{(S_\pi)^{1/2}(1+\beta)}{2\mu} \right].$$

We have assumed that δp is due to the tail of the ρ meson and is therefore very small in our mass range and can be neglected. We have generally taken the form factors to be constant, but have also investigated the effect of allowing \tilde{f}_s to be enhanced. When it has been enhanced we have used the relativistic Watson enhancement factor,

$$\tilde{f}_s = \frac{\tilde{f}_s^0 \sin\delta s}{a_0\beta},$$

where a_0 is in pion Compton wavelengths.

The Monte-Carlo-generated events were subjected to the same cuts as the experimental data (the cuts arise from event-selection criteria to be discussed later). These events were then used to obtain the appropriately modified theoretical distributions of the measured variables, which were then compared with the experimental plots by a χ^2 technique. By changing the values of the input parameters, the gross features of the χ^2 map were studied. However, this procedure, when dealing with four variables, is costly in computer time, and therefore the optimum set of parameters necessary to minimize χ^2 was not obtained by this technique.

B. Second Method

The optimization was performed by a program which simultaneously fitted the $\cos\theta_\pi$, $\cos\theta_l$, ϕ , and $(S_\pi)^{1/2}$ distributions. The sum of the χ^2 for the four distributions was minimized by varying the form factors ν , η , and γ , and the average phase shift $\langle\delta s - \delta p\rangle$. The latter is the average value of $(\delta s - \delta p)$ taken over our mass spectrum. The fit was made to the theoretical one-dimensional plots suitably modified by the Monte Carlo program for the effects of cuts in the data.

For the conditions prevailing in this particular experiment, these modified distributions have the forms given in the Appendix.

C. Third Method

Expression (3) was evaluated for each event and the results were used to construct a likelihood function. A search program was employed to obtain the maximum value of the likelihood as a function of the free parameters, i.e., the form factors and the scattering length. Because of biases introduced in certain variables by the selection criteria, a restricted subset of the data was utilized and the range of integration suitably modified.

D. Fourth Method

Pais and Treiman¹⁶ point out that information on $\langle\delta s - \delta p\rangle$ can be obtained by looking at the average

values of certain I coefficients [Eq. (5)]. This method, unlike the first three approaches, yields information independent of the values of the form factors, and of assumptions regarding their energy dependence. It can be seen that the values of the I 's are governed only by the number of events in various regions of the two-dimensional plot of ϕ versus $\cos\theta_L$.

Specifically, we have

$$\tan\langle\delta s - \delta p\rangle = \frac{1}{2}\langle I_7 \rangle / \langle I_4 \rangle; \quad (11a)$$

also

$$\tan\langle\delta s - \delta p\rangle = 2\langle I_8 \rangle / \langle I_5 \rangle, \quad (11b)$$

where $\langle I_n \rangle$ are defined in Eq. (5).

Should these two expressions for calculating $\langle\delta s - \delta p\rangle$ not yield the same answer, this would mean that (i) time-reversal invariance is violated, (ii) there is an $I=2$ admixture in the s wave, or (iii) there is a significant d -wave π - π contribution.

Furthermore, Pais and Treiman point out that $\langle I_9 \rangle$ should vanish under the assumptions of time-reversal invariance and the $\Delta I = \frac{1}{2}$ rule, and the absence of waves with $l \geq 3$. One may also test the assumption regarding the absence of waves with $l \geq 2$ by examining the $\cos\theta_\pi$ spectrum, which should be fitted by an expression of the form

$$dW/d\cos\theta_\pi = a(1 + b\cos\theta_\pi + c\cos^2\theta_\pi). \quad (12)$$

The need for any additional terms would imply the presence of higher waves.

III. EXPERIMENTAL PROCEDURE

A. Details of Exposure

The beam used was a conventional two-stage separated beam of over-all length approximately 25 m, produced at 15 deg from an internal target in the CERN proton synchrotron. The beam was transported at 800 MeV/c, with a momentum bite of $\pm 1.3\%$, and degraded at the bubble chamber entrance window so that the K^+ stopping points were well spread out in the center of the chamber.

The CERN enlarged 1.1-m-diam heavy-liquid chamber¹⁷ was used. It was filled with C_2F_5Cl , which has a density of 1.2 g/cm³ and a radiation length of 25 cm under operating conditions. In this exposure care was taken to keep the bubble size small in order to be able to see the decay origins clearly. This was also important in seeing the μ^+ from decay of stopping π^+ (range of $\mu^+ = 0.15$ cm).

We took 551 000 pictures, yielding a total of 13.3×10^6 stopping K^+ in the fiducial region (24 stopping K^+ /picture). The film was divided equally between the three institutions (LRL, UW, and UCL) for scanning and preliminary selection of events.

¹⁷ C. A. Ramm and L. Resegotti, in *Proceedings of an International Conference on Instrumentation for High Energy Physics, Lawrence Radiation Laboratory, 1960* (Lawrence Radiation Laboratory, Berkeley, 1961), p. 127.

B. Scanning

The film was scanned for K_{e4} candidates, and approximately two-thirds was rescanned in order to obtain the scanning efficiency. In order to estimate the total number of stopped K^+ every 50th picture was scanned for τ decays.

To pass the preliminary criteria used at the scan table, a K_{e4} candidate had to satisfy four conditions:

(i) The decay point had to lie within the fiducial region. This was a region specified to avoid the immediate vicinity of the beam entry window, which was difficult to scan because of a particularly high density of tracks.

(ii) The ionization of the incoming track near the decay point had to be consistent with that of a stopping K meson.

(iii) There had to be three tracks from the origin.

(iv) One track had to appear to be an electron, identified by spiralization, and the other two had to be consistent with being pions.

These requirements were not very stringent, and 2000 of the events passed by the scanners were measured. The momentum of the electrons was estimated by the Behr-Mittner procedure.¹⁸ Photographic prints of all these events, together with the results of measurement, were then examined by physicists, who applied the more demanding criteria that follow.

C. Selection Criteria for K_{e4}

1. Exclusion of τ Decays at Rest

Most events recorded as candidates by scanners are merely τ decays, for which one of the π^+ is too short to be seen. If this π decays to a μ^+ which then emits an e^+ in approximately the same direction as the μ^+ track, the latter can be mistaken for the first part of the electron track. The electron thus appears to originate from the K^+ decay point. Even though such events outnumber genuine K_{e4} by approximately 5 to 1, they present no problem of identification. This comes about because they are characterized by a π^- and a π^+ going off nearly opposite to each other (at 155–180 deg), and with nearly equal momenta. This configuration, though kinematically allowed for K_{e4} decays, is not particularly favored. Criteria can be set up, then, that exclude these τ decays, while at the same time they reject only a few genuine K_{e4} . These criteria involve measurements on the two long pion tracks. For a τ decay the missing mass, M_N , should be that of a π^+ , viz 139.6 MeV. This estimate will be subject to some measurement error, so in practice one must reject as τ those events with M_N lying in a certain finite range. The extent of this range was determined by plotting M_N for a random sample of K_{e4} candidates (Fig. 2). These events were selected so that the missing momentum was less than 50 MeV/c,

¹⁸ L. Behr and P. Mittner, *Nucl. Instr. Methods* **20**, 446 (1963).

since a π^+ with a momentum exceeding this value would have a range greater than 4.5 mm and its track would be clearly visible even if steeply dipping in the chamber. It is seen that most of the events are centered closely about 139 MeV. On the basis of this figure it was decided to exclude all events for which $130 < M_N < 150$ MeV and at the same time the missing momentum was < 50 MeV/c. This rejected about 1450 events.

2. Exclusion of τ Decays in Flight

Although the candidates had to have an incoming track whose ionization was consistent with the K^+ meson's having come to rest, this requirement does not exclude slow primaries with momenta < 200 MeV/c. A τ decay in flight with a short π^+ track and a μ mistaken as part of the electron track would no longer necessarily have its two visible pions approximately collinear. Thus all candidates were tested to see whether the two pion tracks were consistent with the pions' having come from a τ decay in flight with a K^+ momentum < 200 MeV/c. If so, and if it were further found that the third pion had a momentum < 50 MeV/c, the event was rejected. This criterion affected about 100 events.

3. Kinematical Constraint

For an event to be accepted it did, of course, have to fit satisfactorily the K_{e4} hypothesis. A further 150 events failed to meet this requirement and were rejected. On examination of the prints by a physicist, alternative interpretations were found in all cases.

4. Exclusion of Negative Secondaries with Steep Tracks

For some events, although the negatively charged secondary was consistent with being a pion, there was still some doubt as to its identification. This was the

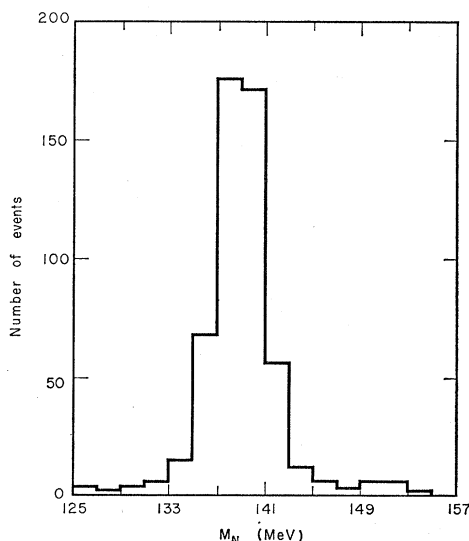


FIG. 2. Missing mass M_N calculated on the basis of measurements on the two pions, for a random sample of K_{e4} candidates. For these events the missing momentum is less than 50 MeV/c.

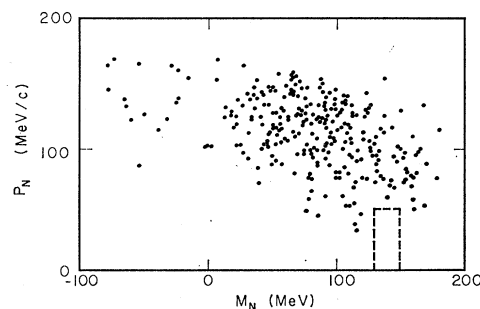


FIG. 3. Scatter plot of the unfitted missing momentum versus missing mass from the two pions, for all accepted K_{e4} . Events in the rectangular region have been excluded by the τ -decay-at-rest criterion.

case when the track was either particularly steep or short. Such a track could be an electron and so when combined with the e^+ would constitute a Dalitz pair. The event would therefore not be a K_{e4} but a τ^+ , $K_{\mu 3}$, or $K_{\pi 2}$.

It was decided in consequence to reject the 21 events for which the negative track had a dip angle > 70 deg.¹⁹

5. Exclusion of Positrons with Steep Tracks

It was sometimes difficult to decide whether a steep track was an e^+ from a K_{e4} decay of a π^+ from a τ decay. Thus all events with an e^+ dipping at an angle > 70 deg were rejected. This accounted for two further events.

6. Exclusion of Pion Secondaries with Short Tracks

As indicated above under subsection 4, a very short π^- (if it did not produce a visible star at the end of its range) could be confused with an e^- . Not so much difficulty was encountered in the identification of a short π^+ , because in general even if the track of the π^+ itself were not visible one could see its decay μ^+ . Nevertheless if either pion had a short track, whether one could unambiguously identify it or not, it was difficult to measure the direction of the track accurately. In the circumstances it was decided to reject the 22 events for which the π^- or the π^+ had a momentum < 48 MeV/c (corresponding to a range of approximately 4 mm).

IV. RESULTS

A. Branching Ratio for $K_{e4}(e^+)$

After application of the various criteria outlined in the previous section, 269 events remain as $K_{e4}(e^+)$ decays. These must be corrected for various losses before the branching ratio can be obtained.

1. Correction for τ -Decay-at-Rest Criterion

Figure 3 shows a scatter plot of the unfitted values of the missing momentum versus the missing mass from

¹⁹ This angle is larger than the previously adopted value (Ref. 1) of 60 deg, because of the more favorable stereo angle of the cameras in the chamber used in this work.

the two pions, for all accepted K_{e4} . No events are to be seen in the rectangular region, owing to the criterion for eliminating τ decays with approximately collinear configuration. The figure demonstrates that the majority of K_{e4} are far removed from this region, and that a correction of only two events should be applied.

The magnitude of this correction has been confirmed by use of the Monte Carlo program previously described.

2. Correction for τ -Decay-in-Flight Criterion

Some K_{e4} at rest have a configuration such that for certain directions for the incoming K meson the event would be thrown out by the τ -decay-in-flight criterion. The K_{e4} found in this experiment were examined with a view to determining the chance that the event would have been rejected had the incoming K meson assumed some other direction. This study led to the conclusion that between 0.5 and 1% of genuine K_{e4} decays had been lost.

3. Correction for π^- Having Steep Tracks

This is a purely geometrical correction based on the solid angle available. Its value is 6.0%.

4. Correction for Positrons Having Steep Tracks

This is also a geometrical correction, but allowance has been made for events having both a steep π^- track and a steep positron track. The correction is 5.6%.

5. Correction for π^\pm Having Short Tracks

The same Monte Carlo program yields a correction of 15% for short π^\pm tracks.

6. Correction for Scanning Efficiency

Based on a rescan of two-thirds of the film, the average efficiency of the first scan was 66% and that of the second scan 73%. This meant that $(83 \pm 5)\%$ of events passing the criteria were found. The events were divided up in various ways according to their configuration, but no preferential bias against any particular type could be discerned.²⁰

7. Other Corrections

No other important means of losing K_{e4} have been found.²¹ There are in addition, however, some correc-

tions to be considered for effects leading to the acceptance of spurious events as genuine K_{e4} .

For example, a τ decay at rest that would normally be rejected by step 1 could be accepted as a K_{e4} if one of the pions scattered very early so that its scattered direction were mistaken for its original direction at the K decay. Consequently a study was made of the visible scatterings to be found on the first 1.5 cm of the tracks associated with events rejected by step 1. This permitted an estimate of the chance that such scatterings could occur in the first 2 mm of the track (and thus escape observation), and of the likelihood that the scatterings would be of a size and in a direction such as to lead to acceptance of the events as K_{e4} . The resulting correction was very small, viz., about one event.

Events normally rejected under 1 have a second way of evading the criterion. This arises when the π^+ decays in flight to give a combined π^+ , μ^+ length significantly greater than the range that the π^+ would have had if it had come to rest. If the π^+ , μ^+ track is mistaken as being entirely due to the π^+ (this is quite likely, as μ^+ from π^+ decay at rest do not always have readily visible tracks in heavy-liquid chambers) the event may be accepted as a K_{e4} . From the moderation times of the pions and the known lifetime it is calculated that one spurious event has been accepted in this manner.

The last background we mention also concerns τ decay. We consider the π^+ to decay while still lightly ionizing and to give a very short track (i.e., the μ^+ goes backwards in the pion center-of-mass system). If the electron from the μ^+ decay is emitted approximately in the same direction as that of the original π^+ , the whole π^+ , μ^+ , e^+ combined track can be mistaken for an e^+ emitted from the K decay. From a consideration of the average moderation time of a pion from a τ decay, the lifetime of the π^+ , the solid angle available to the μ^+ in the pion c.m. system, and the solid angle available to the e^+ , a correction of about one event is indicated.

Several other sources of background were investigated and were found to be small. The over-all result is that our final sample of 269 accepted events contains about three events that are not genuine K_{e4} .

8. Estimation of Total Number of K^+ Based on Scan for τ Decay

The average number of τ decays found in the sample scan of every 50th picture throughout the run was (1.34 ± 0.02) τ /picture. The error is dominated by the statistical uncertainty. The scanning efficiency was determined to be 99.5%. The total number of τ on the 551 000 pictures is

$$551\,000 \times 1.34 \times (100/99.5) = 743\,000.$$

Using the branching ratio²²

$$(K^+ \rightarrow \tau^+)/(\text{all } K^+ \text{ decays}) = (5.57 \pm 0.04)\%,$$

²² See summary by A. H. Rosenfeld *et al.*, Rev. Mod. Phys. **40**, 77 (1968).

²⁰ We used the usual method for determining the scanning efficiency of the two scans, i.e., $\epsilon_1 = N_{12}/N_2$, $\epsilon_2 = N_{12}/N_1$, and $\epsilon_{12} = 1 - (1 - \epsilon_1)(1 - \epsilon_2)$, where N_1 and N_2 are number of events found on the first and second scan, respectively, and N_{12} is the number of events found in common. It has recently been pointed out by S. E. Derenzo and R. H. Hildebrand [Nucl. Instr. Methods (to be published)] that this method, which assumes that each event has the same "visibility," is open to considerable doubt. However, in order to do their analysis three scans of the film are needed. Should the conclusion reached by Derenzo and Hildebrand be applicable to our experiment, the effect would be to lower our value of ϵ_{12} , i.e., to increase the rate.

²¹ In the previous experiment corrections were required for K_{e4} that were unidentified because one of the secondaries left the chamber. Because of the much larger chamber used this time, these corrections are now negligible.

TABLE I. Summary of corrections due to scanning and selection criteria.

Section number	Fractional acceptance
IV A 1	0.993
IV A 2	0.993
IV A 3	0.94
IV A 4	0.944
IV A 5	0.85
IV A 6	0.83
IV A 7	1.011
Product	0.624

one finds total number of $K^+ = (13.3 \pm 0.3) \times 10^6$.

9. Estimation of Branching Ratio

After application of the various corrections, the estimated total number of $K_{e4}(e^+)$ is 431 (see Table I). The branching ratio is therefore

$$K_{e4}(e^+)/\text{all } K^+ \text{ decays} = (3.25 \pm 0.35) \times 10^{-5}.$$

This compares well with the value $(3.6 \pm 0.8) \times 10^{-5}$ found in the previous experiment.¹ The corresponding decay rate is $(2.60 \pm 0.30) \times 10^3 \text{ sec}^{-1}$.

B. Upper Limit to Branching Ratio for $K_{e4}(e^-)$ Decay

No candidates for the $K_{e4}(e^-)$ mode were found, either in this or in the previous experiment.¹

Although the scanning criteria for this mode were similar to those for $K_{e4}(e^+)$, the detection efficiencies for the two modes are not equal. The sources of background are different, so one cannot make a straight comparison.

For example, a $\pi^- \rightarrow \mu^- \rightarrow e^-$ decay is less probable, so corrections IV A 1 and IV A 2 can be relaxed.

Instead of rejecting one of the pions—viz. the negative one—when its track is steep, we now under IV A 4 must reject *either* π^+ if its track is steep. This is because

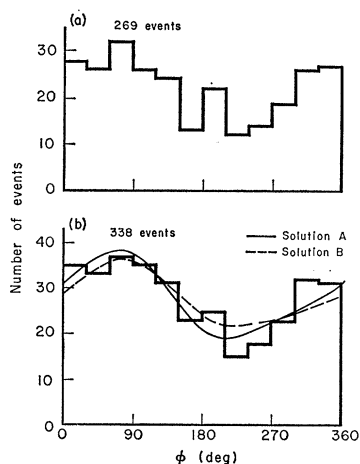


FIG. 4. Distribution of the angle ϕ . (a) For this experiment; (b) for both experiments combined.

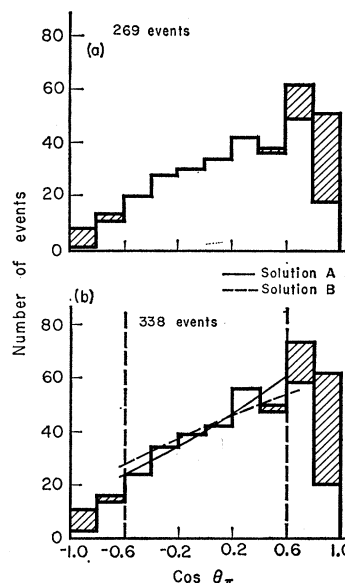


FIG. 5. Distribution of the angle θ_π . (a) For this experiment; (b) for both experiments combined. The cross-hatched events show the extent of the correction needed for the short-track-pion criterion. Only events lying within the range $-0.6 < \cos \theta_\pi \leq +0.6$ are used in the over-all fit.

the π^+ may be ambiguous with an e^+ and the K decay could then be a τ' with a Dalitz electron pair.

Events must be rejected if the two π^+ are consistent with having come from a τ decay and the e^- lies in approximately the direction of the expected third pion. This is necessary to avoid a τ decay in which the π^- charge-exchanges, and one of the γ from the π^0 decay gives a Compton electron almost immediately, the combined π^-, e^- track appearing to be an e^- from the K decay.

Considerations of this nature lead to an over-all detection efficiency for $K_{e4}(e^-)$ which is 70% of that appropriate for $K_{e4}(e^+)$.

Thus this experiment yields an upper limit

$$K_{e4}(e^-)/\text{all } K^+ \text{ decays} < 7 \times 10^{-7}$$

at the 95% confidence level.

C. Mass and Angular Distributions

Figure 4(a) shows the distribution of ϕ , the angle between the dipion and dilepton planes. Figure 4(b) gives the same distribution with the events from the previous experiment included. Both are adequately fitted by a function of the form $\alpha(1 + \beta \cos \phi + \gamma \sin \phi + \delta \sin^2 \phi)$, where for Fig. 4(b) $\beta = 0.20 \pm 0.08$, $\gamma = 0.26 \pm 0.08$, and $\delta = -0.03 \pm 0.11$. The value of χ^2 is 3.5 for 8 deg of freedom. (The curves shown refer not to this solution but to solutions involving simultaneous fits to several histograms. These are described later.)

The angle that the π^+ makes with the dipion line of flight in the dipion rest system is plotted in Fig. 5. Unlike ϕ , $\cos \theta_\pi$ is strongly affected by the cut on short-

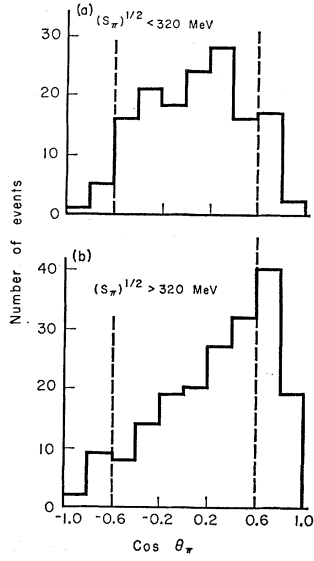


FIG. 6. Distribution of θ_π , uncorrected for the loss of short-track pions. (a) For events with $(S_\pi)^{1/2} < 320$ MeV; (b) for events with $(S_\pi)^{1/2} > 320$ MeV.

track pions. An impression of the size of the corrections needed to each bin is given by the cross-hatched events. These were estimated by the Monte Carlo program (mentioned in Sec. II), which generated K_{e4} events by using our most probable set of values of the form factors and the π - π phase shift (to be obtained in Sec. IV D).

The $\cos\theta_\pi$ distribution should be of the form $a(1+b\cos\theta_\pi+c\cos^2\theta_\pi)$. From Fig. 5(b), we estimate b to be (0.61 ± 0.12) . Evaluation of the coefficient c depends sensitively upon the numbers of events with large values of $|\cos\theta_\pi|$. These are the values for which

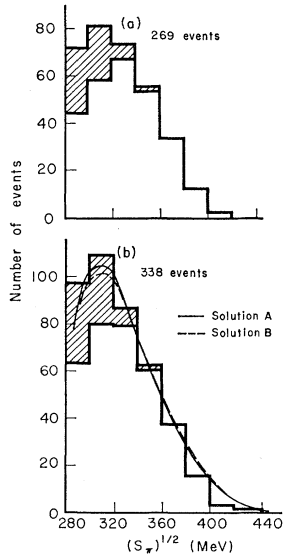


FIG. 7. Distribution of the invariant mass of the dipion system. (a) For this experiment; (b) for both experiments combined. The cross-hatched events show the extent of the correction needed mainly for the criterion excluding short pions.

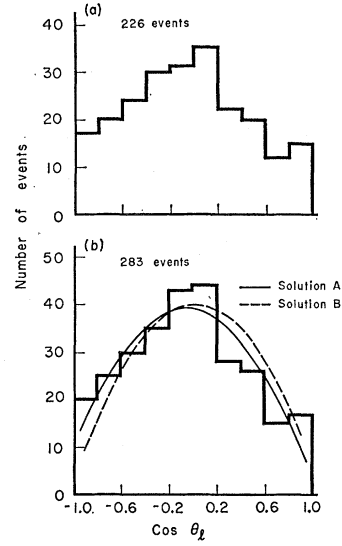


FIG. 8. Distribution of the angle θ_l . (a) For this experiment; (b) for both experiments combined. Events with $\beta_{ev} > 0.95$ have been excluded from these histograms.

the correction for short-track pions is greatest, and so it is difficult to estimate c with any degree of reliability. We have considered it desirable to base conclusions to be drawn later from this distribution solely on that part which is largely unaffected by the cut, i.e., the region lying between the dashed lines.

It can be seen from Fig. 6 that the slope of the $\cos\theta_\pi$ plot changes markedly as a function of S_π . This behavior can be understood if the f_p form factor goes to zero as β goes to zero at small values of S_π . The quantity $[(\beta X/M^2)\tilde{f}_p']$, which replaces \tilde{f}_p in the analysis to allow for the effects of the angular momentum barrier, has just this kind of behavior.

Figure 7 shows the invariant-mass distribution of the dipion system. The cross-hatched events in the first three bins have been added to compensate for the loss of short pions. Similarly the estimated two events excluded by the τ -decay-at-rest criterion (Sec. IV A 1) are kinematically constrained to fall within the fourth bins.

Figure 8 gives the histogram of $\cos\theta_l$, the angle between the e^+ and the dilepton line of flight in the dilepton rest frame. $\cos\theta_l$ is largely unaffected by the short-track pion correction, but for this angle a new effect becomes significant. It concerns events for which the laboratory-system velocity β_{ev} of the dilepton system is close to unity. For this class of events the errors on $\cos\theta_l$ arising from measurement errors on angles and momenta can become highly asymmetric. This introduces a systematic bias as events are moved more readily towards negative values of $\cos\theta_l$ than towards positive ones. This effect is readily reduced to negligible proportions by removing the 16% of events for which $\beta_{ev} > 0.95$. This cut explains why the numbers of events in Fig. 8 are less than those for the other plots.

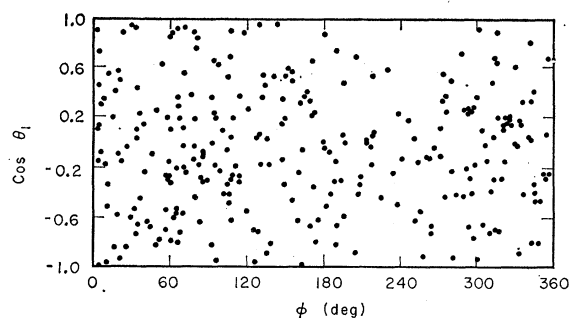


FIG. 9. Scatter plot of $\cos\theta_l$ versus ϕ for both experiments combined. Events with $\beta_{ev} > 0.95$ have been excluded.

Figure 9 is a two-dimensional scatter diagram showing the correlation between $\cos\theta_l$ and ϕ , for events with $\beta_{ev} < 0.95$. As was indicated in Sec. II, correlations between these two angles have a particular significance in the Pais-Treiman method of analysis. The average values of the relevant correlations are shown in Table II.

It is to be noted that the quantity $\langle \sin^2\theta_l \sin 2\phi \rangle$, which determines $\langle I_9 \rangle$, is consistent with zero, as is required by time-reversal invariance.

D. Determination of π - π Phase-Shift Difference and Form Factors

In principle, the most satisfactory way of determining the s -wave $I=0$ π - π phase shift is to use the ratios of the I coefficients given in Eq. (11). The theory upon which such estimates are based rests on very few assumptions, viz., the absence of d waves and of an $I=2$ admixture in the s wave, and time-reversal invariance.

Unfortunately the correlations concerned are not very strong, and the statistical accuracy obtainable with 300 events is exceedingly poor. We are not even able unambiguously to determine the sign, as both expressions (11a) and (11b) involve quantities (viz., I_4 and I_8) which are not significantly different from zero. Taking the data at face value, the estimates of the magnitude of $\langle \delta s - \delta p \rangle$

$$|\langle \delta s - \delta p \rangle| = \tan^{-1}(\frac{1}{2}\langle I_7 \rangle / \langle I_4 \rangle) = 90 \pm 40 \text{ deg}$$

and

$$|\langle \delta s - \delta p \rangle| = \tan^{-1}(2\langle I_8 \rangle / \langle I_6 \rangle) = 0 \pm 40 \text{ deg}.$$

One observation we can make, however, is that $\langle I_7 \rangle$, and consequently the numerator of expression (11a), is almost 3 standard deviations from zero. [Note that the errors as quoted in (13) are not Gaussian.] Thus although the large fractional error on the denominator makes it difficult to establish a magnitude for $\tan\langle \delta s - \delta p \rangle$, our result is not easily reconcilable with a value close to zero.

Until it becomes possible to perform experiments yielding larger numbers of events, the above method for extracting the phase shift is not very promising, so in order to proceed further we need to introduce values

TABLE II. Mean values of the ϕ versus θ_l correlations relevant to the determination $I_1 \cdots I_9$.

$\langle \cos 2\theta_l \rangle$	-0.502 ± 0.035
$\langle \sin^2\theta_l \cos 2\phi \rangle$	-0.011 ± 0.034
$\langle \sin 2\theta_l \cos \phi \rangle$	-0.001 ± 0.028
$\langle \sin \theta_l \cos \phi \rangle$	$+0.093 \pm 0.036$
$\langle \cos \theta_l \rangle$	-0.048 ± 0.029
$\langle \sin \theta_l \sin \phi \rangle$	$+0.102 \pm 0.036$
$\langle \sin 2\theta_l \sin \phi \rangle$	-0.004 ± 0.028
$\langle \sin^2\theta_l \sin 2\phi \rangle$	-0.041 ± 0.033

for the form factors, and assumptions regarding their energy dependence.

As mentioned in Sec. II, three methods of obtaining acceptable sets of values for the form factors and phase-shift difference have been used. They each have certain advantages. The maximum-likelihood technique is able to extract information contained in correlations between the different variables. This information is lost in performing a simultaneous least-squares fit to the histograms of ϕ , $\cos\theta_\pi$, $\cos\theta_l$, and $(S_\pi)^{1/2}$. However, this second method is able to make use of events with $|\cos\theta_\pi| > 0.6$ and $\beta_{ev} > 0.95$ in those plots where they introduce no bias. The Monte Carlo method, on the other hand, is the most effective way of checking the influence of cuts and biases in the data.

Assuming all form factors to be independent of S_π and S_l , the least-squares-fit program yields four solutions with acceptable values of χ^2 . These are listed in Table III.

Nominally there are 29 degrees of freedom. However, the fact that the same events are used in all histograms imposes restrictions that tend to reduce the effective number of degrees of freedom. By fitting 50 batches of Monte Carlo events generated with solution A parameters, and examining the resulting χ^2 values, we estimate that the effective number of degrees of freedom to which the χ^2 values of Table III refer lies between 28 and 29. This implies that these histograms are almost independent projections. In considering the results of Table III, it should be noted that the Pais-Treiman form factor f_p may be obtained from the value of ν by multiplying it by ≈ 0.11 .

With the maximum-likelihood program we can in fact exclude solutions C and D. This is rendered possible by a study of θ_l versus ϕ correlations, which are not open to examination by the program that performs a fit to the one-dimensional plots. Specifically, it is found that the large values of γ and of $\sin\langle \delta s - \delta p \rangle$ lead to values of I_8 which are 3 to 4 standard deviations removed from the experimental number.

Of the two remaining solutions, A is somewhat favored over B, but both have acceptable χ^2 values. Unfortunately, with respect to determining the phase shift, although the two solutions have the same magnitude for $\langle \delta s - \delta p \rangle$, the signs are opposite. We postpone discussion of this point until later in the paper.

TABLE III. Values of the form factors and phase shifts for the four solutions with acceptable χ^2 (\tilde{f}_s unenhanced).

	Solutions			
	A	B	C	D
\tilde{f}_s^a	4.32 ± 0.26	4.52 ± 0.29	4.25 ± 0.33	4.14 ± 0.32
\tilde{g}	-6.96 ± 0.77	6.01 ± 0.86	1.06 ± 0.60	-2.36 ± 0.65
\tilde{h}	-10.4 ± 3.8	-4.92 ± 3.67	-42.5 ± 8.3	-42.2 ± 8.5
\tilde{f}_p'	54.0 ± 6.1	-14.0 ± 5.1	21.7 ± 9.5	41.4 ± 9.3
$\eta (\equiv \tilde{g}/\tilde{f}_s)$	-1.61 ± 0.15	1.33 ± 0.17	0.25 ± 0.14	-0.57 ± 0.15
$\gamma (\equiv \tilde{h}/\tilde{f}_s)$	-2.41 ± 0.86	-1.09 ± 0.81	-10.0 ± 1.8	-10.2 ± 1.9
$\nu (\equiv \tilde{f}_p'/\tilde{f}_s)$	12.5 ± 1.2	-3.1 ± 1.1	5.1 ± 2.2	10.0 ± 2.1
$\langle \delta s - \delta p \rangle$ (rad)	-0.44 ± 0.14	0.44 ± 0.15	1.21 ± 0.10	-1.17 ± 0.10
$a_0 (\chi_\pi)$	-0.89 ± 0.28	$1.26_{-0.52}^{+0.68}$	Very large	$-2.83_{-0.50}^{+0.40}$
χ^2	26.6	38.6	36.3	26.0

^a We have used the value of 0.26 for $\sin\theta_e$ [N. Brene, M. Ross, and A. Sirlin, Nucl. Phys. **B6**, 256 (1968)] in order to obtain these values.

We have also investigated the effect of an S_π energy dependence in \tilde{f}_s proportional to the Watson enhancement factor, and solutions corresponding to solutions A and B in Table III are given as solutions A_e and B_e in Table IV. The differences are not large.

The maximum-likelihood method yielded essentially the same solutions, within errors, and the Monte Carlo approach also located the two minima in the χ^2 map in regions corresponding closely to solutions A and B.

V. DISCUSSION

The rate for $K_{e4}(e^+)$ decay has been found to be $(2.60 \pm 0.30) \times 10^3 \text{ sec}^{-1}$. Theoretical calculations that do not include final-state interactions all contain an adjustable parameter, and can be brought into agreement with our rate with a reasonable value of the parameter. Brown and Faier⁹ allow for the final-state interactions by assuming that the decay proceeds through a σ meson. Although their rate is in agreement with our value, the $(S_\pi)^{1/2}$ spectrum does not furnish any evidence of the presence of a σ meson. Weinberg,¹¹ using current algebra and soft-pion techniques, is able to relate the K_{e4} form factors to those of K_{e3} , and hence predicts a rate of $(1.88 \pm 0.23) \times 10^3 \text{ sec}^{-1}$. In regard to

this, however, we point out that for solution A, where ν is large, f_p contributes $\approx 30\%$ to the rate.

The upper limit, at the 95% confidence level of 7×10^{-7} for the $K_{e4}(e^-)$ branching ratio, adds weight to the $\Delta Q = \Delta S$ rule. $K_{e4}(e^-)$ decay, if it occurs, proceeds through the axial-vector current. $K_{e4}(e^+)$ decay involves a mixture of both axial-vector and vector, but although the latter gives rise to strong interference terms, its contribution to the rate is small. Thus our conclusions refer specifically to the rule as it applies to the axial-vector currents in weak interactions. In interpreting our result one must be careful to make allowance for the differing dipion interactions in $K_{e4}(e^-)$ decay and in $K_{e4}(e^+)$ decay. For $K_{e4}(e^-)$ the dipion state is pure $I=2$, whereas for $K_{e4}(e^+)$ we have $I=0$ or 1. Because of the relatively low energy of the interaction, one further assumes only s and p waves to be important in $K_{e4}(e^+)$, whereas only s waves would be present in $K_{e4}(e^-)$. The violation parameter is defined as the ratio of the amplitudes of the currents,

$$x = A(\Delta Q = -\Delta S) / A(\Delta Q = +\Delta S).$$

In order to evaluate x one needs to know the enhancement factor due to the final-state interaction. For no s -wave interaction our branching ratios lead to < 0.15 at the 95% confidence level, whereas for enhancement factors variously estimated as extending up to a value of 4 (Refs. 8 and 10) we obtain

$$x < 0.3 \text{ (95\% confidence level)}.$$

The three methods that yielded values for both the form factors and the phase-shift difference agreed that there are two acceptable solutions.

We should mention that in the paper based on the previous experiment¹ a single unambiguous solution was reported. This was because the importance of the $\cos\theta_l$ distribution and the form factor f_p had not at that time been recognized. The differing conclusions of that paper and this, it should be stressed, are not due to any contradiction between the two sets of data, but rather to the method of analysis now including the f_p form factor. For the same reason, the analyses given in the

TABLE IV. Values of the form factors and phase shifts corresponding to solutions A and B of Table III when \tilde{f}_s is enhanced.

	Solutions	
	A_e	B_e
\tilde{f}_s^a	4.08 ± 0.23	6.1 ± 0.66
\tilde{g}	-6.77 ± 0.74	6.8 ± 1.09
\tilde{h}	-9.35 ± 3.42	-5.02 ± 3.89
\tilde{f}_p'	52.2 ± 5.8	-14.7 ± 5.7
$\eta (\equiv \tilde{g}/\tilde{f}_s)$	-1.66 ± 0.15	1.12 ± 0.13
$\gamma (\equiv \tilde{h}/\tilde{f}_s)$	-2.29 ± 0.83	-0.82 ± 0.63
$\nu (\equiv \tilde{f}_p'/\tilde{f}_s)$	12.8 ± 1.2	-2.41 ± 0.90
$\langle \delta s - \delta p \rangle$ (rad)	-0.28 ± 0.12	0.50 ± 0.10
$a_0 (\chi_\pi)$	-0.58 ± 0.24	1.50 ± 0.48
χ^2	31.8	33.0

^a We have used the value of 0.26 for $\sin\theta_e$ [N. Brene, M. Ross, and A. Sirlin, Nucl. Phys. **B6**, 256 (1968)] in order to obtain these values.

first three preliminary reports² of this experiment are to be regarded as inadequate.

That we should have obtained two solutions that fit the data is not entirely unexpected. Berends, Donnachie, and Oades²³ have pointed out that if the original type of analysis proposed by Cabibbo and Maksymowicz¹³ were applied to the $(S_\pi)^{1/2}$, $\cos\theta_\pi$, and ϕ data with the modification that f_p were no longer put to zero, then one must obtain two solutions that are equally satisfactory. These are related to each other in the following way:

$$\begin{aligned} {}_1\tilde{f}_s &= {}_2\tilde{f}_s, \\ {}_1\tilde{f}_p &= {}_2\tilde{f}_p + \xi {}_2\tilde{g}, \\ {}_1\tilde{g} &= -{}_2\tilde{g}, \\ {}_1\tilde{h} &= {}_2\tilde{h}, \\ {}_1\langle\delta s - \delta p\rangle &= -{}_2\langle\delta s - \delta p\rangle, \end{aligned}$$

where ξ is a kinematic factor, having an approximate value of 9.5, and is appropriate to our particular method of introducing an angular momentum barrier effect for f_p . They went on to point out that this ambiguity could be resolved by studying the variable θ_l . Specifically the two solutions lead to coefficients for the $\cos\theta_l$ term that are equal in magnitude but opposite in sign.

An essential conclusion of this experiment is that the information contained in our θ_l plot is insufficient to distinguish which solution is correct. The two possible values of the coefficient of $\cos\theta_l$ are -0.09 and $+0.03$. The experimental value is -0.14 ± 0.09 .

Thus although our experiment favors the former value, we would be unwise to consider this solution as established. The need for such caution is particularly emphasized by the fact that by allowing \tilde{f}_s to be enhanced we can materially alter the relative probabilities of the two solutions. Nevertheless, certain definite statements can be extracted from the data.

The most statistically significant angular correlation is the slope of the $\cos\theta_\pi$ plot, which was seen in Sec. IV C to have a value 0.61 ± 0.12 . This slope is governed by the values of ν and η , and our measurement leads to the approximate relation

$$2\nu + 9\eta = 7,$$

which holds when the magnitudes of the form factors and phase shift are not greatly in excess of those of solutions *A* and *B*.

It is clear from this relation that if ν could be determined, the value of η would be established and consequently \tilde{g} . The ambiguity of the two solutions would then be resolved. However, ν has little significance for the other angular distributions and has essentially to be determined from the $\cos\theta_\pi$ distribution.

Next we note that both solutions require the vector form factor \tilde{h} ($\gamma = \tilde{h}/\tilde{f}_s$) to be significantly different from zero, and its sign is negative. It is true that in solution *B* it is not so far removed from zero. However,

the poorer χ^2 for this solution is largely due to an internal conflict in the data in which the large value of \tilde{h} required by the coefficient of $\cos\phi$ is set against other requirements of the fit. Thus γ for this solution has already been reduced to a level that makes the over-all probability less than that of solution *A*. That \tilde{h} is significant is a conclusion that was not justified on the statistics of the previous experiment.

Finally, we point out that the quantity $\eta \sin\langle\delta s - \delta p\rangle$ is a constant for both types of solution given by Berends, Donnachie, and Oades, a change of sign of η being compensated by a similar change in $\sin\langle\delta s - \delta p\rangle$. This constant relationship is seen to hold true for the two solutions *A* and *B*, and also the solutions in which \tilde{f}_s is enhanced, *A_e* and *B_e*. The values of the product are respectively (0.68 ± 0.22) , (0.57 ± 0.20) , (0.46 ± 0.20) , and (0.56 ± 0.13) . The quantity is almost entirely governed by the coefficient of $\sin\phi$.

Weinberg¹¹ estimates $\sin\delta s = 0.1$ (giving $a_0 = 0.2\chi_\pi$) and $\eta = 1$, using current algebra. His value for the product is thus 0.1. His requirement of a positive value for η leads to a choice of solutions *B* or *B_e*. Our evaluation of the product $\eta \sin\langle\delta s - \delta p\rangle$ is thus just over two standard deviations from his estimate.

In conclusion, we consider the possibility of resolving the two-solution ambiguity in later experiments. In principle, the ideal way to extract the phase shift is to use either Eq. (11a) or (11b). This, as Pais and Treiman have explained, could yield estimates independent of assumptions regarding the form factors. That we were not able even to obtain the sign of the phase shift in this experiment was because our statistics were inadequate to obtain values of I_8 or I_4 that were significantly removed from zero.

Likewise the sign of the phase shift was unresolved in the alternative approach because of the smallness of the coefficient of $\cos\theta_l$, which is related to I_6 . Indeed, in order to make an unambiguous measurement of $\langle\delta s - \delta p\rangle$ it is necessary to determine that one of the odd moments of $\cos\theta_l$, I_4 , I_6 , or I_8 is significantly different from zero. It should be noted that, this being the case, the problem is not merely one of accumulating larger statistics. The θ_l plot, as we have pointed out, is liable to suffer from biases arising from measurement inaccuracy. Increased measuring errors in any subsequent experiment would of course render it necessary to make even more drastic cuts in $\beta_{e\pi}$ than the one employed in this investigation.

ACKNOWLEDGMENTS

We express our deep gratitude to the CERN personnel, and especially to Dr. C. A. Ramm and his colleagues in the N.P.A. Division for making this exposure possible. We should like to acknowledge the help of Dr. R. W. Birge, Dr. W. M. Powell, and Dr. D. J. Miller during the early part of this work. We also acknowledge many helpful discussions on the theoretical

²³ F. A. Berends, A. Donnachie, and G. C. Oades, Phys. Rev. **171**, 1457 (1968).

cal aspects of the work, especially those with Dr. A. Pais, and Dr. R. Cence, Dr. S. Treiman, Dr. A. Donnachie, Dr. G. Oades, Dr. S. M. Berman, and Dr. J. Yellin. The members of the University College London group thank the Science Research Council for its financial support, and one of them (W.L.K.) acknowledges the receipt of a Turner & Newall fellowship. The work of the Lawrence Radiation Laboratory group was done under auspices of the U. S. Atomic Energy Commission.

APPENDIX

These are the equations used in the simultaneous fit to the ϕ , $\cos\theta_\pi$, $\cos\theta_l$, and $(S_\pi)^{1/2}$ histograms. The expressions include corrections appropriate to the selection criteria adopted in this investigation.

ϕ Distribution

$$\partial\Gamma/\partial\phi = \alpha(1 + \beta \cos\phi + \lambda \sin\phi + \kappa \cos^2\phi),$$

where

$$\begin{aligned}\alpha &= 56.3/(2 + \kappa), \\ \beta &= -12.38\gamma \cos\langle\delta s - \delta p\rangle M, \\ \lambda &= 60.7\eta \sin\langle\delta s - \delta p\rangle M, \\ \kappa &= (0.29\gamma^2 - 8.9\eta^2)M,\end{aligned}$$

$$M = (127 + 0.37\nu^2 + 23.3\eta^2 + 0.14\gamma^2 + 3.68\eta\nu)^{-1}.$$

$\cos\theta_\pi$ Distribution

$$\partial\Gamma/\partial \cos\theta_\pi = a(1 + b \cos\theta_\pi + c \cos^2\theta_\pi),$$

where

$$\begin{aligned}a &= 246/(6 + 0.72c), \\ b &= (33\nu + 162.5\eta) \cos\langle\delta s - \delta p\rangle L, \\ c &= (1.81\nu^2 + 33.5\eta^2 - 0.46\gamma^2 + 18.1\eta\nu)L,\end{aligned}$$

and

$$L = (154 + 14.4\eta^2 + 0.46\gamma^2)^{-1}.$$

$\cos\theta_l$ Distribution

$$\partial\Gamma/\partial \cos\theta_l = A(1 + B \cos\theta_l + C \cos^2\theta_l),$$

where

$$\begin{aligned}A &= 28.3/(1 + 0.333C), \\ B &= -4.9\eta\gamma N, \\ C &= (-190 - 0.552\nu^2 - 7.9\eta^2 + 0.21\gamma^2 - 5.52\eta\nu)N, \\ N &= (190 + 0.552\nu^2 + 21.3\eta^2 + 0.21\gamma^2 + 5.52\eta\nu)^{-1}.\end{aligned}$$

and

$(S_\pi)^{1/2}$ Distribution

$$\begin{aligned}280-300 \text{ MeV: } & (122 + 0.23\nu^2 + 6.3\eta^2 + 0.10\gamma^2 + 1.92\eta\nu)F, \\ 300-320 \text{ MeV: } & (135 + 0.53\nu^2 + 18.7\eta^2 + 0.26\gamma^2 + 4.90\eta\nu)F, \\ 320-340 \text{ MeV: } & (108 + 0.54\nu^2 + 23.3\eta^2 + 0.28\gamma^2 + 5.50\eta\nu)F, \\ 340-360 \text{ MeV: } & (73 + 0.40\nu^2 + 21.0\eta^2 + 0.21\gamma^2 + 4.42\eta\nu)F, \\ 360-380 \text{ MeV: } & (43 + 0.21\nu^2 + 15.2\eta^2 + 0.12\gamma^2 + 2.69\eta\nu)F, \\ 380-400 \text{ MeV: } & (21 + 0.07\nu^2 + 8.9\eta^2 + 0.06\gamma^2 + 1.19\eta\nu)F, \\ 400-420 \text{ MeV: } & (9 + 0.014\nu^2 + 4.1\eta^2 + 0.01\gamma^2 + 0.35\eta\nu)F, \\ 420-440 \text{ MeV: } & (3 + 0.007\nu^2 + 1.4\eta^2 + 0.004\gamma^2 + 0.15\eta\nu)F,\end{aligned}$$

where

$$F = (1.25 + 0.0051\nu^2 + 0.264\eta^2 + 0.003\gamma^2 + 0.055\eta\nu)^{-1}.$$